Journal of
Materials Chemistry B

Accepted Manuscript

This article can be cited before page numbers have been issued, to do this please use: T. Shao, T. Liu, H. Liu, M. Zhang, Y. Shen, A. Gao, X. Tian, Q. Zhang, J. Wu and Y. Tian, *J. Mater. Chem. B*, 2019, DOI: 10.1039/C9TB00421A.

ROYAL SOCIETY OF CHEMISTRY

rsc.li/materials-b

View Article Online
DOI: 10.1039/C9TB00421A

Journal Name

ARTICLE

Identify fatty liver diverse stage by a two-photon absorption triphenylamine-based BODIPY analogues

Received 00th January 20xx,
Accepted 00th January 20xx

DOI: 10.1039/x0xx00000x

www.rsc.org/

Tao Shao[†a], Tianyan Liu[†b], Hui Liu[†a], Mingzhu Zhang[a], Yu Shen[a], Awei Gao[a], Xiaohe Tian[b], Qiong Zhang[a], Jieying Wu[a], Yupeng Tian[*a]

Fatty liver disease (FLD) is one of the major health hazards against people's health, while its effective and accurate detection during different phase is still problematic. Herein, four BODIPY analogues (**01B~04B**) with different donor/acceptor group were rational designed for such purpose. Within them, the photophysical and theoretical study demonstrated that **03B** has an obvious intramolecular charge transfer (ICT) with the two-photon action cross-sections up to 198 GM in the near-infrared region. The initial *in vitro* assessment indicated that **03B** could interact with the lipid substances with significant fluorescence enhancement. Due to its high biocompatibility, lipid-affinity and sensitivity, **03B** can be targeted 3T3-L1 model cells at different FLD induced stages. Further in vivo study was demonstrated that **03B** could clearly distinguish FLD tissue and display the lesion *in situ*. These results offered a promising optical tool for FLD evaluation among different phases and monitoring dynamics at sub-cellular level.

Introduction

Fatty liver (FL) is a serious threat to people's health as it affects the progression of other chronic liver diseases and participate in the pathogenesis of type 2 diabetes and atherosclerosis.[1] Since FL is reversible and can be recovered by early diagnosis and treatment, sensitive detection methodology remains vital important to prevent its further progress. At present, there have been three methods for fatty liver diagnosis, including ultrasonography, Computed Tomography (CT) scanning and liver biopsy.[2] However, ultrasonography and (CT) scanning may be misdiagnose as showing malignant liver masses because steatosis is diffuse in most patients with fatty liver disease.[3] On the premise of ensuring accuracy, liver puncture is the first choice whereas liver puncture spend too much time on experiment. Overall, the above-mentioned treatment often brought side effect as well as time consuming. Therefore, it is urgent to develop a rapid approach to diagnosis.

Small fluorescent probes remain as a powerful tool for medical diagnosis, bio-labelling, chemical detection. In particular, BODIPY analogues, as an excellent fluorescent dye,[4] have been used in various fields, such as chemosensors,[5] fluorescent switches[6] and labelling reagents.[7, 8] Due to their remarkable properties[9] including high photophysical stability,[10] high fluorescence quantum yield[11] and large absorption extinction coefficients,[12] they were widely used in biological research as fluorescent probes.[13] For example, BODIPY can be used as a mitochondrial polarity probe in live cells[14] and lysosome-targeting probe.[15] BODIPY493/505 also can be used Lipid drop probe. However, the lipid drop probe with two-photon property for FL diagnoise purpose is rarely reported. Two-photon absorption (2PA) materials have been reported for deep penetration and avoiding auto-fluorescence of back-ground, which is very important advantage for bioimaging and biomedical research.[16]

With this goal in mind, we designed and synthesized a series of novel D-π-A type BODIPY analogues (**01B**~**04B**). The N, N-diethyl group was used as electron donor in order to enhance ICT, which was in favor of generating 2PA activity and lipid solubility. Furthermore, triphenylamine as the electron acceptor group in the designed molecule (**03B**) could greatly enhance two-photon absorption properties. Besides, **03B** was highly lipophilic and can be stained 3T3-L1 cells (mouse fibroblasts). Tissue imaging of **03B** showed that the two-photon fluorescence intensity was increased in fatty liver tissue. The results might give guidance to design novel two-photon fluorescent BODIPY analogues with multiple functions.

Experimental section

Materials and apparatus

All chemicals were obtained commercially and solvents were purified with conventional methods before using. The ^{1}H (400 MHz) and ^{13}C (100 MHz) NMR spectra were collected on a Bruker Avance 400 spectrometer at 25 °C (TMS as internal standard in NMR). Coupling constants J were given in Hertz. FT-IR spectra were

[a] College of Chemistry and Chemical Engineering, Key Laboratory of Functional Inorganic Materials Chemistry of Anhui Province, and Anhui Province Key Laboratory of Chemistry for Inorganic/Organic Hybrid Functionalized Materials, Anhui University, Hefei 230039, P. R. China.
[b] School of Life Science, Anhui University, Hefei 230601, PR China.
*Corresponding author. Fax: +86-551-63861279; Tel: +86-551-63861279
E-mail address: yptian@ahu.edu.cn
†These authors contributed equally to this work and should be considered co-first authors

obtained in the solid (KBr disk) on a NEXUS-870 (Nicolet) spectrophotometer in the 400 ~ 4000 cm^{-1}. Mass spectra were performed on a Micromass GCT-MS (ESI source). Absorption spectra were recorded on a UV-3100 spectrophotometer. Emission spectra were obtained on an F-2500 fluorescence spectrophotometer.

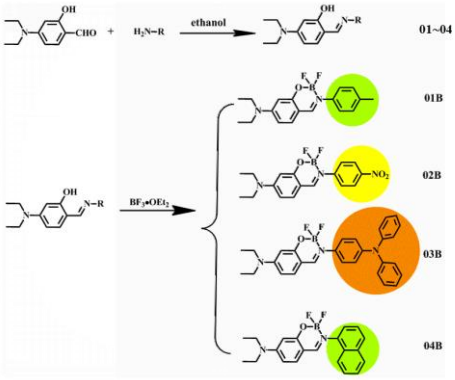

Scheme 1 The synthetic routes of BODIPY analogues.

Synthesis

Synthesis of 01B

The BODIPY analogues were prepared according to the similar procedures with previous work.[17-19] **01** (0.4 g, 1.5 mmol) was added in freshly distilled CH_2Cl_2 (15 mL) and was heated to dissolution. Then $BF_3{\cdot}OEt_2$ (0.47 mL 3.75 mmol)was added by using injector, waiting for a minute, DIEA (0.65 mL 3.75 mmol) was added, the solution was heated to reflux for 2 h, cooled the room temperature and poured into saturation solution of $NaHCO_3$ (50 mL), the aqueous layer was extracted with dichloromethane and the organic phases were dried (anhydrous Na_2SO_4). The solvent removed and the residue separated by column chromatograph (using silica gel) giving a yield of 0.32 g (64.6 %); ^{1}H NMR (400 MHz, $CDCl_3$) δ (ppm): 8.02 (s, 1H), 7.38 (d, J = 8.20 Hz, 2H), 7.23 (t, J = 12.43 Hz, 3H), 6.34 (dd, J = 2.27 Hz, 9.03 Hz, 2H), 6.23 (s, 1H), 3.44 (q, J = 7.12 Hz, 4H), 2.37 (s, 3H), 1.25 (t, J = 7.40 Hz, 6H). ^{13}C NMR (100 MHz, $CDCl_3$) δ (ppm): 161.76, 158.09, 156.08, 140.79, 137.61, 133.74, 129.92, 122.98, 106.47, 98.17, 45.12, 29.69, 21.00, 12.64. ESI-MS: m/z, cal: 330.17, found: 331.17 $[M+1]^+$. FT−IR (KBr, cm^{-1}): 2978.98 (w), 2925.81 (w), 1626.26 (s), 1591.59 (s), 1507.52 (s), 1447.44 (w),1354.83 (m), 1277.87 (w), 1205.94 (s), 1143.80 (m), 1074.12 (w), 1038.38 (m), 972.61 (m),901.32 (w), 822.92 (w), 795.56 (w), 493.77 (w).

Synthesis of 02B

The synthesis of **02B** was similar to that of **01B**, except **01** was replaced by **02**. Yield: 0.42 g (75.7 %); ^{1}H-NMR (400 MHz, $CDCl_3$) δ (ppm): 8.28 (s, 1H), 8.06 (d, J= 9.1 Hz, 4H), 7.67 (d, J= 8.91 Hz, 1H), 6.41(dd, J= 2.23, 9.15 Hz, 1H), 6.21 (s, 1H), 3.48(q, J= 7.15 Hz, 4H), 1.19(t, J= 7.41 Hz, 6H). ^{13}C NMR (100 MHz, $CDCl_3$) δ (ppm): 162.52, 157.32, 152.49, 146.68, 139.21, 134.58, 126.34, 124.97, 113.38, 107.75, 97.71, 45.43, 13.38. ESI-MS: m/z, cal: 361.14, found: 362.1477 $[M+1]^+$. FT-IR (KBr, cm^{-1}): 3481.73(m), 3361.58(m), 3219.96(w), 2923.51(m), 2853.06(w), 1629.50(s), 1583.27(s), 1505.28(m), 1479.95(m), 1446.04(w), 1333.96(s), 1300.21(s), 1216.36(m), 1146.02(w), 1112.38(m), 1036.80(m), 841.30(m), 752.77(m), 631.90(m).

Fig. 1 Structures of BODIPY analogues.

Synthesis of 03B

03 (0.87 g, 2.0 mmol) was added mixture solution of ethyldiisopropylamine (DIEA)（0.5 mL）and dichloromethane (10 mL), it was stirred at the room temperature for 30 minutes under the nitrogen protection. Then $BF_3{\cdot}OEt_2$（2.52 mL, 20 mmol）was added by using injector. The reaction at room temperature for 18 h. EtOH was added when the reaction was finished. The rude production was collected by filtration; the product was separated by column chromatography (using silica gel). Yield:0.52 g (53.8 %). ^{1}H NMR (400 MHz, $CDCl_3$) δ (ppm): 8.03 (s, 1H), 7.36 (d, J= 8.59 Hz, 2H), 7.25 (m, 5H), 7.07 (m, 7H), 6.36 (d, J= 9.02 Hz, 1H), 6.25 (s, 1H), 3.44 (q, J= 7.02 Hz, 4H), 1.25 (t, J=7.1 Hz, 6H). ^{13}C NMR (100 MHz, d_6-DMSO) δ (ppm):161.60, 157.39, 147.36, 137.50, 133.61, 129.38, 124.67,123.49, 106.52, 45.18, 13.39. ESI-MS: m/z, cal: 483.23, found: 484.2401$[M+1]^+$. FT-IR (KBr, cm^{-1}): 3036.53(w), 2924.37(m), 2851.73(w), 1636.72(s), 1596.89(s), 1508.10(s), 1492.48(s), 1461.05(w), 1414.55(w), 1355.51(m), 1327.68(m), 1276.60(m), 1213.79(m), 1145.70(m), 1033.43(m), 971.51(m), 826.80(m), 745.65(m), 695.34(m), 616.91(m).

Synthesis of 04B

The same procedure as described synthesis of **02B**, except **01** was replaced by **04**. Yield: 0.44 g (80.1 %). ^{1}H NMR (400 MHz, $CDCl_3$) δ(ppm): 7.90 (m, 4H), 7.52 (m, 4H), 7.18 (d, J = 8.99 Hz, 1H), 6.37 (dd, J = 2.07, 9.00 Hz, 2H), 6.32 (s, 1H), 3.47 (q, J = 7.13, 7.13, 7.15 Hz, 4H), 1.24 (t, J = 0.40 Hz, 6H). ^{13}C NMR (100 MHz, $CDCl_3$) δ(ppm): 161.94, 156.05, 139.17, 133.94, 128.32, 124.85, 123.14,105.05, 97.42, 45.19, 30.11, 12.65. ESI-MS: m/z, cal: 366.17, found: 367.1783$[M+1]^+$. FT-IR (KBr, cm^{-1}): 2922.83(m), 1623.20(s), 1591.17(s), 1506.85(s), 1450.51(s), 1411.46(m), 1344.58(s), 1216.58(m), 1077.74(m), 964.78(m), 824.68(m), 787.31(m), 678.28(m).

X-ray crystallography and structure solution

X-ray diffraction data of single crystals were collected by Siemens Smart 1000 CCD diffractometer, and the determination of unit cell parameters and data collections were performed with MoK_α radiation (λ = 0.71073 Å). Unit cell dimensions were collected with least-squares refinements and all structures were solved by direct methods using SHELXS-97. The other non-hydrogen atoms were located in successive difference Fourier syntheses. The final refinement was performed by full-matrix least-squares methods with anisotropic thermal parameters for non-hydrogen atoms on F^2. The hydrogen atoms were added theoretically and riding on the concerned atoms.

View Article Online
DOI: 10.1039/C9TB00431A

Computation detail

The ground states for each molecule were carried out with B3LYP functional employing a 6–31G* basis set, Internal coordinate constraints or no symmetry were applied during optimization. The absorption energies were investigated by time-dependent density functional theory (TD–DFT). All calculations were performed by the use of the Gaussian 03 suite of programs.

Nonlinear optical property

2PA cross–section of BODIPY derivatives were obtained by the two–photon excited fluorescence (2PEF) method with femtosecond laser piles and a Ti:sapphire system (680–1080 nm, 80 MHz, 140 fs) as the light source (the concentration of BODIPY analogues were 1 $\times 10^{-3}$ M in THF). The fluorescence quantum yields (Φ) were determined by using fluorescein as the reference according to the literature method. The σ value of compound BODIPY analogues were determined to that of fluorescein by the following equation:

$$\sigma = \sigma_{ref} \frac{\Phi_{ref}}{\Phi} \frac{c_{ref}}{c} \frac{n_{ref}}{n} \frac{F}{F_{ref}}$$

where the subscripts ref stands for the reference molecule. σ is the 2PA cross-section value, c is the concentration of solution, n is the refractive index of the solution, F is the integrated area of the detected two-photon-induced fluorescence signal, and Φ is the fluorescence quantum yield. The σ_{ref} value of reference is taken from the literature.

Cell culture

Cells (including cancer cell and normal cell) were cultured in 25cm^2 culture flasks in DMEM, supplemented with fetal bovine serum (10 %), penicillin (100 units/mL) and streptomycin (50 units/mL) at 37 ^oC in a CO_2 incubator (95 %relative humidity, 5 % CO_2). Cells were seeded in 35 mm glass bottom cell culture dishes, at a density of 1 × 10^5 cells and were allowed to grow when the cells reached more than 60 % confluence.

Cytotoxicity assay

To ascertain the cytotoxic effect of BODIPY analogues treatment over a 24 h period, the **01B-04B** methylthiazolyldiphenyl-tetrazolium bromide (MTT) assay was performed. HepG2 cells were grown to ~ 70 % confluence in 96–well plates before treatment. Prior to the compounds' treatment, the growth medium was refreshed, and L was first dissolved in DMSO to 1 mM and then diluted twice by DMEM cell culture medium to obtain the final concentrations. The treated cells were incubated for 24 h at 37 °C and under 5 % CO_2. Subsequently, the cells were treated with 5 mg/mL MTT solution (10 μL/well) and incubated for an additional 4 h (37 °C, 5 % CO_2).Then, MTT solution was removed and the formazan crystals were dissolved in DMSO (100 μL/well). The absorbance at 490 nm was recorded. The cell viability (%) was calculated according to the following equation: cell viability % = OD_{490} (sample) / OD_{490} (control)×100, where OD490 (sample) represents the optical density of the wells treated with various concentrations of the compounds and OD_{490} (control) represents that of the wells with only DMEM + 10 % FCS. Three independent trials were conducted, and the averages and standard deviations are plotted. The reported cell survival percent are relative to untreated control cells.

Differentiation induction of 3T3-L1

3T3-L1 cell was seeded in 24-well culture plate at the concentration of 2*10^5 cells per well and the contact inhibition needs to be continued for 2 days after full fusion. Cells were treated in induced solution (I) that is DMEM high glucose medium comprising s 0.5 mmol/L IBMX, 1 μmol/L dexamethasone, 10 mg/L insulin and 10 % FBS for 2 days, and turn to use of 10 mg/L insulin and 10% FBS containing 10 mg/L DMEM sugar medium induced solution (II) for two days. Then cells were cultured in DMEM sugar medium containing 10 % FBS and change the fluid every two days. After 4 days the most preadipocytes into mature fat cells which can be used for next test.

Tissue staining

Mouse tissues (liver, heart, brain) were extracted and put into 4 % paraformaldehyde for 3-5 days then dehydrated in 30 % sucrose solution. Tissue slices (20 μm) were obtained by Leica CM3050S freezing microtome. The slices were stained with complexes (100 μM) for 30 min at 37 ^oC in 95 % air 5 % CO_2, then washed with PBS buffer 3 times. Tissue was mounted cover-slipped using NucRed™Live647, and imaged directly using a Leica TCS SP8 confocal microscopy.

Two-photon imaging and co-localization with living cell

HELF, HepG2 and 3T3-L1 cell was chosen to use in confocal microscopy imaging. The cells were plated in 24 well glass-bottom plates and cultured for 48 h. The cells were solely incubated with 1 mL media/DMSO (v/v=99:1) containing various concentrations of compounds for 30 min (37 °C, 5 % CO_2). The excess complexes were washed away by PBS for 3 times, after that the confocal microscopy imaging was carried out. For co-localization, the cells were incubated with ER-tracker Red (Ex=587nm, Em=615nm), Mito-

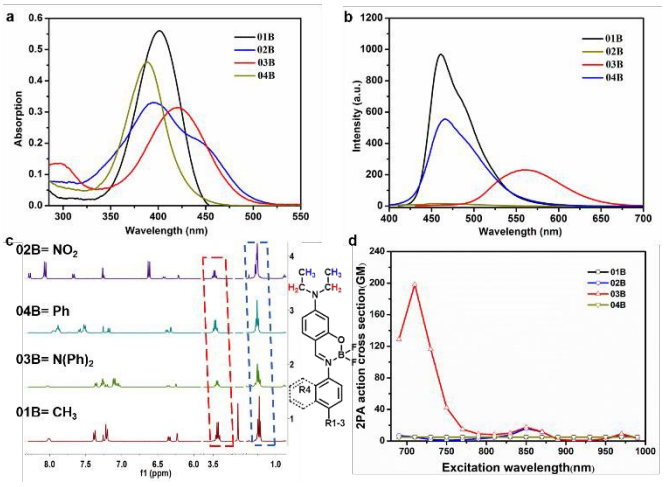

Fig. 2 a-b): The linear absorption and emission spectra of (**01B**~**04B**) in DMSO ($\times 10^{-5}$ M) ; c): ^{1}H NMR of (**01B**—**04B**) in $CDCl_3$; d) The active 2PA cross-section of **01B**—**04B**.

View Article Online
DOI: 10.1039/C9TB00421A

tracker Deep Red (Ex=644nm, Em=665nm), NucRed™Live647(Ex=647nm, Em=660nm) and for 10 min after washed way the excess tracker by PBS for 3 times. Cells were imaged using confocal laser scanning microscopy using oil immersion lenses.

Image processing and analysis

Micrographs were processing and analyzed by Huygens software and ImageJ 1.48 v (32-bit). Quantification of the fluorescence intensity was achieved via Analyze >> Tools >> ROI manager in ImageJ from three parallel experiments. Quantification of single cell intensity profile was achieved via Analyze >> Plot Profile by selecting one cell in ImageJ. Quantification of colocolization coefficency was achieve via an external plugin via Plugins >> Colocolization Finder. For more details, please refer to online sources: https://imagej.nih.gov/ij/

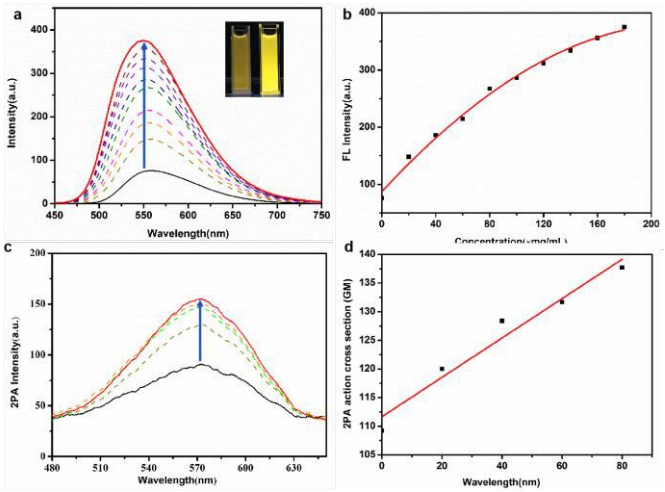

Fig. 3 a) One-photon fluorescence emission spectra of compound **03B** (10 μM in PBS buffer, pH = 7.4) upon addition of liposome (0—180 μg/mL) b) plot of the emission intensity at 550 nm as a function of additives concentration.; c) two-photon fluorescence emission spectra of compound **03B** (100 μM in PBS buffer, pH = 7.4) upon addition of liposome (0—80 μg/mL) d) plot of the two photon cross section at 570 nm.

Results and discussion

Photophysical properties

The chemical structures and detailed synthetic processes were highlighted in **Fig. 1** and **Scheme 1**. The linear absorption and fluorescence spectra of **01B**~**04B** were given in **Fig. 2a** and **Fig. 2b**. All BODIPY analogues are located around 400 nm. Wavelength order of maximum absorption are **03B** (416 nm) > **01B** (395 nm) > **02B** (385 nm) ≈ **04B** (384 nm). The calculated excitation energies of four complexes at low-energy bonds were 3.17 eV (**01B**), 3.26 eV (**02B**), 2.95 eV (**03B**) and 3.21eV (**04B**) in **Fig. S1**, respectively, which provided a satisfactory explanation on the obvious red shift of **03B** compared to **01B**, **02B** and **04B**. And the absorption spectra of **03B** showed no significant solvation effect in **Fig. S5**. For fluorescence spectra, **03B** is located around 560 nm, which showed large Stock's shift (150 nm) compared to other BODIPY analogues. It can be explained by charge transfer tendency with different terminal groups. The N, N-diethyl group was used as the strong electron donor, and the triphenylamine as the electron acceptor group which can be achieved the energy matching with the donor group (N, N-diethyl), leading to greatly enhance linear and nonlinear optical signal. As showed in **Fig. S6**, the intensity of the fluorescence of **03B** in different solvents also showed slight solvation effect which depends on the stability of the excited state. The fluorescence quantum yield of **03B** is little difference which was consistent with the trend of the fluorescence intensity. To further clarify the terminal groups effect on molecules, ^{1}H NMR experiments were carried out. The signals of N, N-diethyl group are gradually moved to low-field (**Fig. 2c**). The order of chemical shift was **02B** > **04B** > **03B** > **01B**. The TD-DFT calculations (**Fig. S1**) showed that was exist obvious ICT compare to **02B**, **01B** and **04B**, which can cause better 2PA activity of **03B**.[20, 21] Next, we studied the two-photon absorption properties of **01B**~**04B** (**Fig. 2d**). The active two-photon absorption cross section of **03B** (198 GM) is 13.2 times of **02B** (15 GM). It can be explained by two reasons. (1) **03B** has a higher degree of charge transfer than other molecules. (2) the crystal structure of **01B** and **04B** were showed weak force (**Fig. S3**). There were existing C-H···F hydrogen bonds between the **01B**, **02B** and **04B** molecules, respectively. For **03B**, the terminal triphenylamine group shows with a special spatial configuration. The intermolecular hydrogen bonds can be avoided due to the increased molecules distance. Therefore, there are fewer non-radiative transitions in **03B**, resulting in stronger two-photon fluorescent intensity.

Fluorescent sensing behavior of 03B towards lipid

In order to examine the potential ability of **03B** for lipid targeting, a screening experiment was initially carried out using DNA, RNA, lecithin, liposome. As shown in **Fig. S9**, **03B** displayed an obvious fluorescence intensity increase tendency by adding lipid (lectin or liposome). The titration of liposome was then carried out by semi–quantitative assessment in **Fig. 3a**. It can be clearly seen that the fluorescence intensity increases 5-fold upon increasing the concentration of liposome from 0 μg/mL to 180 μg/mL (**Fig. 3b**). The two-photon fluorescence intensity was increased for 1.7 times (**Fig. 3c**), and the two-photon cross section was increased for 1.3 times with addition of liposome from 0 μg/mL to 80 μg/mL (**Fig. 3d**). The fluorescence intensity was different with various liposome concentration which may be due to their different luminescence mechanism. These results showed that **03B** can be as a 2PA probe sensing liposome.

Mechanism studies

In order to investigate lipid targeting mechanism, log P was tested to evaluate cell uptake and localized, where P is the partition coefficient between octanol and water. As showed in **Table. S5**, the order of log P were **01B** (2.88) >**03B** (1.55) > **04B** (1.37)>**02B** (0.87). For lipid-localized, **03B** (1.55) was the most suitable one with lipophilicity values around 2.[22] TD-DFT was calculation further assistance to prove that there exists interactions between **03B** and lipid. It can be seen that the electrons of **03B** were mainly distributed in Schiff base part (**Fig. 4a**). Hence, we can speculate

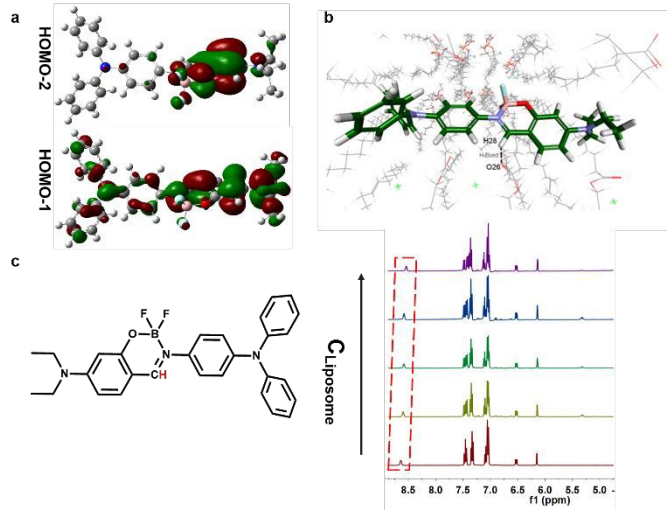

Fig. 4 a) TD-DFT calculations of **03B** (HOMO-1, HOMO-2). b) Molecular docking mode of **03B** treated with lipid bilayer. c) ^{1}H-NMR spectra of **03B** treated with liposome.

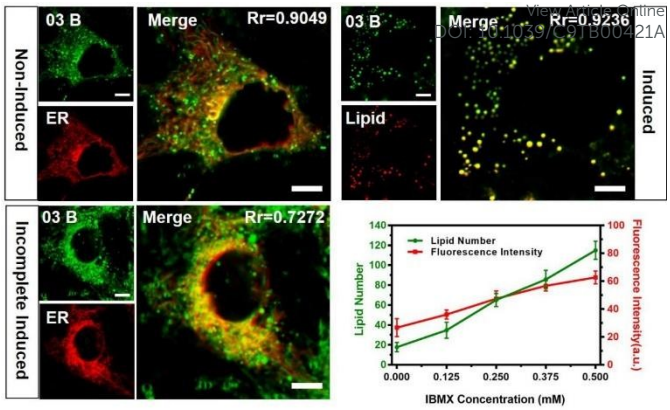

Fig. 5 Two-photon fluorescence microscopy imaging of **03B** stained on 3T3-L1 cells before and after induction (scale bars = 20 μm, concentration=10 μM, λ_{ex}=710 nm, λ_{em} = 550 nm).

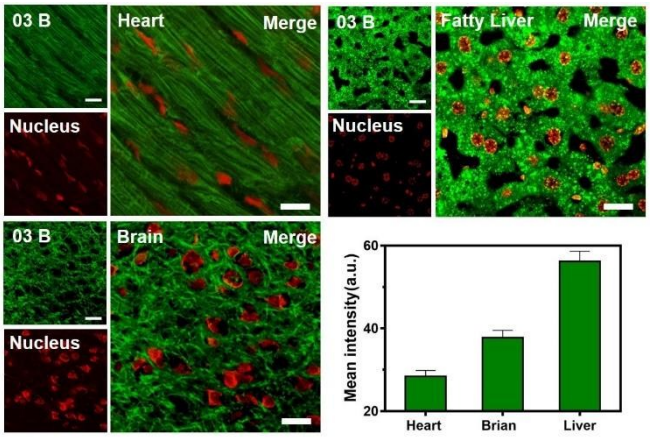

Fig. 6 2PFM imaging of **03B** for fatty liver tissue tissue imaging and mean intensity in tissue (scale bars = 20 μm, concentration=10 μM, λ_{ex} = 710 nm, λ_{em} = 550 nm).

that the Schiff base part is the site of lipid reaction. Furthermore, molecular docking experiments were performed to verify the above sensing mechanism.[23] The docking results indicated that **03B** were enriched mainly in the lipid bilayer, which might due to that **03B** can interact with the base of the lipid bilayer *via* hydrogen bonds. **Fig. 4b** showed that the H28 (the double bond of Schiff base) interact with O26 in lipids. To further confirm the mechanism, ^{1}H NMR titration experiments were carried out as an effective tool (**Fig. 4c**).[24] H_a on the Schiff base moves gradually to the up-field, indicating that **03B** can be interacted with lipid. Considering the above research, the binding site between **03B** and lipid is the H of Schiff base.

Lipophihicity and cellular uptake of 03B

Consider the lipid is an enclosed vesicle with bilayer structure. We speculated that **03B** may interact with lipotropic parts in lipid. As **03B** is a lipophilic molecule interacting strongly with liposome *in vitro*, it is proposed that **03B** possesses potential to target an area rich in lipid, which was addressed through detailed in living cell studies.

A co-staining experiment using Mito-Tracker Deep Red and ER-Tracker green was performed to further determine whether **03B** was internalized with membrane-rich organelle endoplasmic reticulum. The results showed that **03B** can be stained in ER region (person's coefficient = 0.88 in **Fig. S11**). **Fig. S12** suggesting **03B** could associate with lipophilic regions in different type of cells including HepG2 cells (liver hepatocellular cells), HELF cells (human embryonic lung fibroblasts), 3T3-L1 cells (mouse fibroblasts).

Herein in this work, **03B** as lipophilic two-photon active BODIPY derivatives was further applied to identify differentiated 3T3-L1 Adipocytes. It is found that during varying degrees of induction of3T3-L1 cells according to the IBMX (3-isobutyl-1-methyl-7H-xanthine) concentration, **03B** was displayed diverse intracellular distribution pattern (**Fig. 5**). At non-induced control group, the probe was highly overlapped with endoplamic reticulum. Further incomplete induced cells using mild IBMX treatment showed much less association between the probe and ER compartment. While a clear vesicular cytosolic distribution was clearly observed, indicating the probe was partially internalized with the lipid drop. It is worthy note that in the complete induced experiment, all the probe was highly overlapped with Nile Red stained lipid-drop units with a considerable Pearson correlation coefficient (Rr = 0.92).

The above real time results suggested that the small organic molecule **03B** was extremely lipophilic molecule in fat cells.

2PFM imaging of 03B for fatty liver tissue

Encouraged by the above results, we sought to investigate the ability of **03B** visualize the fatty liver tissues. Subsequently, fresh tissue slices including heart, brain and fatty liver were stained by incubating with 100 μM **03B** for 30 min. As shown in **Fig. 6** the micrographs and later intensity analysis, brain signal displayed greater intensity due to its higher lipid composition[25] among all the organs. For a sharp contrast, fatty liver slices stained with **03B** show significant brighter two-photon fluorescence signal, again proved the selectivity and sensitivity of this probe against FLD tissue.

Conclusion

For summary, four novel BODIPY derivatives (**01B**~**04B**) based on the N–B–O pattern have been simply and efficiently synthesized. **03B** has outstanding photophysical and biological properties below. (1) **03B** has large Stokes Shifts (150 nm) and moderate two-photon cross section of two-photon. (2) **03B** interact with the lipid substances with significant fluorescence enhancement (3) **03B** can distinguish adipocytes at different induced stages. (4) **03B** can stain fatty liver with strong two-photon fluorescence intensity. Thus, we are envisioned that the present work will provide important information to researchers engaged in developing such novel materials to detect fatty liver and imaging in adipocytes.

Conflicts of interest

There are no conflicts to declare.

Acknowledgment

This work was supported by the National Natural Science Foundation of China (51432001, 21602003, 51672002, 21871003, 51772002), Anhui Provincial Natural Science Foundation of China (1708085MC68), and Anhui University Doctor Startup Fund (J01001962), the Higher Education Revitalization Plan Talent Project (2013).

References

1. M. Y. Donath and S. E. Shoelson, *Nature Reviews Immunology*, 2011, **11**, 98.
2. S. B. Reeder and C. B. Sirlin, *Magnetic Resonance Imaging Clinics*, 2010, **18**, 337-357.
3. C. Valls, R. Iannacconne, E. Alba, T. Murakami, M. Hori, R. Passariello and V. Vilgrain, *European Radiology*, 2006, **16**, 2292-2308.
4. A. Loudet and K. Burgess, *Chemical Reviews*, 2007, **107**, 4891-4932.
5. N. Boens, V. Leen and W. Dehaen, *Chemical Society Reviews*, 2012, **41**, 1130-1172.
6. S. Kolemen and E. U. Akkaya, *Coordination Chemistry Reviews*, 2018, **354**, 121-134.
7. T. Kowada, H. Maeda and K. Kikuchi, *Chemical Society Reviews*, 2015, **44**, 4953-4972.
8. R. Subiros-Funosas, L. Mendive-Tapia, J. Sot, J. D. Pound, N. Barth, Y. Varela, F. M. Goñi, M. Paterson, C. D. Gregory, F. Albericio, I. Dransfield, R. Lavilla and M. Vendrell, *Chemical Communications*, 2017, **53**, 945-948.
9. H. Gao, Y. Gao, C. Wang, D. Hu, Z. Xie, L. Liu, B. Yang and Y. Ma, *ACS Applied Materials & Interfaces*, 2018, **10**, 14956-14965.
10. F. Bergström, I. Mikhalyov, P. Hägglöf, R. Wortmann, T. Ny and L. B. Å. Johansson, *Journal of the American Chemical Society*, 2002, **124**, 196-204.
11. Y. Zhou, Y. Xiao, S. Chi and X. Qian, *Organic Letters*, 2008, **10**, 633-636.
12. T. Yogo, Y. Urano, Y. Ishitsuka, F. Maniwa and T. Nagano, *Journal of the American Chemical Society*, 2005, **127**, 12162-12163.
13. H. Zhu, Z. Zhang, S. Long, J. Du, J. Fan and X. Peng, *Nature protocols*, 2018, **13**, 2348-2361. View Article Online DOI: 10.1039/C9TB00421A
14. X. Li, X. Tong, Y. Yin, H. Yan, C. Lu, W. Huang and Q. Zhao, *Chemical Science*, 2017, **8**, 5930-5940.
15. M. Li, J. Fan, H. Li, J. Du, S. Long and X. Peng, *Biomaterials*, 2018, **164**, 98-105.
16. D. Zhang, Y. Wang, Y. Xiao, S. Qian and X. Qian, *Tetrahedron*, 2009, **65**, 8099-8103.
17. M. Baruah, W. Qin, N. Basarić, W. M. De Borggraeve and N. Boens, *The Journal of Organic Chemistry*, 2005, **70**, 4152-4157.
18. T. W. Hudnall and F. P. Gabbaï, *Chemical Communications*, 2008, DOI: 10.1039/B808740G, 4596-4597.
19. M. Zhang, R. Su, Q. Zhang, L. Hu, X. Tian, Y. Chen, H. Zhou, J. Wu and Y. Tian, *Sensors and Actuators B: Chemical*, 2018, **261**, 161-168.
20. K. Pal, I. Samanta, R. K. Gupta, D. Goswami and A. L. Koner, *Chemical Communications*, 2018, **54**, 10590-10593.
21. X. Tian, Q. Zhang, M. Zhang, K. Uvdal, Q. Wang, J. Chen, W. Du, B. Huang, J. Wu and Y. Tian, *Chemical Science*, 2017, **8**, 142-149.
22. C. Caporale, C. A. Bader, A. Sorvina, M. G. Kdm, B. W. Skelton, T. A. Gillam, P. J. Wright, P. Raiteri, S. Stagni and J. L. Morrison, *Chemistry - A European Journal*, 2017, **23**.
23. Y. Tang, M. Kong, X. Tian, J. Wang, Q. Xie, A. Wang, Q. Zhang, H. Zhou, J. Wu and Y. Tian, *Journal of Materials Chemistry B*, 2017, **5**, 6348-6355.
24. Y. Shen, T. Shao, B. Fang, W. Du, M. Zhang, J. Liu, T. Liu, X. Tian, Q. Zhang, A. Wang, J. Yang, J. Wu and Y. Tian, *Chem Commun (Camb)*, 2018, **54**, 11288-11291.
25. K. D. Foust, E. Nurre, C. L. Montgomery, A. Hernandez, C. M. Chan and B. K. Kaspar, *Nature Biotechnology*, 2008, **27**, 59.

View Article Online
DOI: 10.1039/C9TB00421A

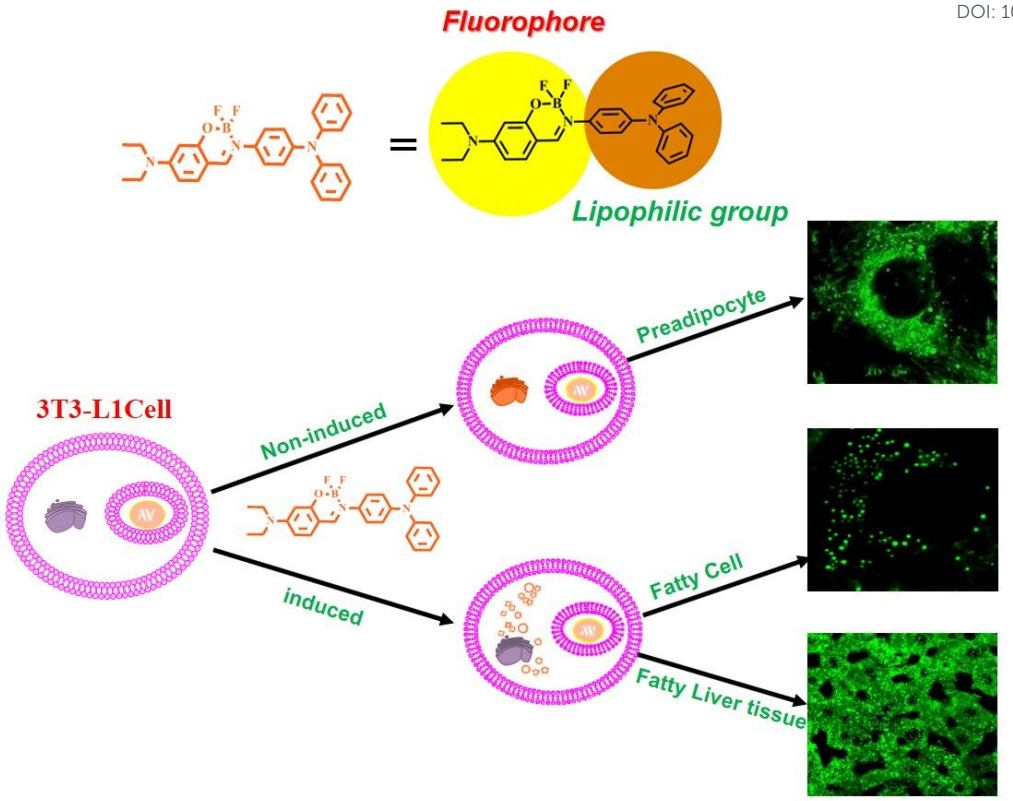

TOC synopsis: 03B could be targeted 3T3-L1 model cells at different FLD induced stages and could clearly distinguish FLD tissue and display the lesion *in situ*. These results offered a promising optical tool for FLD evaluation among different phases and monitoring dynamics at sub-cellular level.